Supplementary Materials and Methods

Molecular determinants of U-type inactivation in Kv2.1 channels

Yen May Cheng, John Azer, Christine M Niven, Pouya Mafi,
Charlene R Allard, Ji Qi, Samrat Thouta, and Thomas W Claydon

Western Blotting

Xenopus oocytes were prepared and injected with RNA in the same manner as described for whole-cell current recordings. Two-days post injection, the expression levels of wt and E352C Kv2.1 channels were measured using two-electrode voltage clamp recordings of whole-cell currents. Whole cell lysates were extracted as described previously by Juranka et al. (1). Briefly, 8 oocytes were resuspended in 12 µl lysis buffer (150 mM NaCl, 10 mM K_2HPO_4, 500 µM phenylmethanesulfonylfluoride, pH 7.4, 1% Triton X-100, supplemented with protease inhibitor cocktail (Sigma P2714)) for 5 min on ice and homogenized by gentle grinding with a glass rod. Cell homogenates were centrifuged for 15 min (13,000 rpm at 4°C) and the crude protein samples (aqueous layer) were retrieved for subsequent use in Western blotting. Equal amounts of the protein samples were treated with either water (non-reducing) or 1 mM DTT (reducing) at room temperature for 30 min (2-4). The samples were then loaded in a 1:1 ratio of SDS-containing loading buffer (25 mM Tris base, 192 mM Glycine, 0.1% SDS) onto a standard 5% stacking and 10% resolving SDS-PAGE gel. Following electrophoresis, the separated proteins were transferred to a nitrocellulose membrane, which was then blocked for 1 h in 4°C blocking solution (1% non-fat dried milk powder in TBS-T buffer containing 10 mM Tris base, 150 mM NaCl, 0.1% Tween-20). The membrane was subsequently incubated overnight at 4°C with a 1:200 dilution of anti-Kv2.1 antibody (C-terminal epitope; Alomone Labs Ltd, Jerusalem, Israel) in blocking solution. The membrane was then washed three times (10 min each) with TBS-T buffer, followed by a 1 h incubation at room temperature in blocking solution supplemented with a 1:10,000 dilution of secondary antibody (horseradish peroxidise-conjugate of goat-anti rabbit IgG; Santa Cruz Biotechnology) at room temperature. The membrane was washed a further three times, after which protein was detected using an enhanced-chemiluminescence detection kit (Immun-Star HRP Chemiluminescent Kit, Bio-Rad, Missisauga, Ontario, Canada). Unless otherwise stated, reagents were obtained from Sigma-Aldrich, except for the SDS and Tween-20, which were from Bio-Rad.

Figure S1. The putative interaction between E352C and C232 is very specific. To assess whether E352C could interact with cysteine residues at locations other than C232 in S2, we examined the effect of substituting cysteine residues for L225 (*A*), V228 (*B*), and F236 (*C*) in the background of the E352C/C232V double mutation. *Panels A-C* show the inactivation-voltage relationships of each of these triple mutants, respectively, under control conditions (i.e. ND96, ●) and following a 30 min treatment with 1 mM DTT (○). Each mutant shows, unlike the E352C (C232) construct, distinct U-type inactivation behaviour under control conditions. Additionally, while there is some enhancement of the maximum extent of inactivation, DTT treatment does not drastically increase the U-type inactivation behaviour of these mutants, unlike its effects on the E352C (C232) mutant (see Figure 3). The results indicate that E352C cannot interact with cysteine residues substituted at these three positions and support the conclusion that the removal of U-type inactivation by E352C is dependent on the availability of C232 for disulfide bond formation. In each panel, data points represent mean ± S.E.M. of at least 5 oocytes.

Figure S2. wt and E352C mutant Kv2.1 channels expressed in *Xenopus* oocytes do not form dimers. *Xenopus* oocytes injected with wt- and E352C Kv2.1 channel RNA were solubilised and subjected to Western blot analysis using a Kv2.1 specific antibody. The panel shows images from a representative Western blot (n = 3) of proteins isolated from oocytes injected with the indicated cRNA. As a negative control, samples were run alongside a crude protein sample isolated from 20 uninjected oocytes (uninj.). Also indicated is whether or not the protein sample was subjected to DTT treatment (− or + DTT). The position of Kv2.1 α-subunit monomers is indicated by the black arrowhead, along with relevant molecular size standards. wt Kv2.1 subunits appeared as monomers of approximately 100 kDa, as has previously been shown (4). For both the wt and E352C mutant channel, we did not observe dimers at the expected size of 217 kDa (shown with a white arrowhead; 4), but rather monomers, which suggests that the channel subunits do not form inter-subunit interactions. Consistent with this, neither wt nor E352C subunits were affected by pre-treatment with DTT.

Figure S3. Characterization of wt Kv2.1 gating. *A*, macroscopic currents recorded from an oocyte expressing wt Kv2.1 in ND96 showing current activation. Current (*bottom*) was elicited by 300 ms depolarizations from −80 mV to +60 mV, in 10 mV increments (*top*). Tail currents were recorded at −40 mV for 50 ms before returning to the −80 mV holding potential. *B*, G-V curve for wt Kv2.1. The normalized conductance at each test voltage was calculating by normalizing the tail current amplitudes to the maximum tail current amplitude. The solid line represents a fit of the data to a Boltzmann function. Data points represent the mean ± S.E.M. from 9 cells; $V_{1/2}$ and k were −1.6 ± 1.2 mV and 9.8 ± 0.3 mV, respectively. *C*, time constants for current activation at different membrane potentials were obtained by fitting the rising portion of macroscopic currents to a single exponential. *D*, the time course of channel deactivation was studied by measuring the voltage dependence of the decay of tail currents. Channels were activated by a 500 ms conditioning pulse to +60 mV, after which the voltage was stepped to between −40 and −140 mV in 10 mV (*top*). The holding potential was −80 mV and current recordings were performed in 30 mM K^+_o to increase the amplitude of the inward tail currents at very negative potentials. *Inset*, tail currents are shown at higher magnification. *E*, the time course of channel deactivation was quantified by fitting tail currents such as those in *D* to a double exponential function with time constants $\tau_{deact,\ fast}$ (●) and $\tau_{deact,\ slow}$ (○). *F and G*, the time course of recovery from inactivation was determined from current records such as that shown in *G*. After recovery from an initial control pulse to +60 mV, inactivation was induced by application of a 5 s pulse train (40 ms pulses to +60 mV from −80 mV, with a cycle length of 80 ms). Recovery from inactivation was then monitored by applying, after a variable interval at −120 mV, a test pulse to +60 mV. *Panel G* shows 9 superimposed traces where the interval between the inactivation pulse train and the test pulse doubled with every sweep, starting with an interval of 100 ms. The time constant for current recovery (τ_{rec}) was determined by fitting the relationship between the normalized recovery current and the recovery time at −120 mV to a single exponential function (*solid line, Panel F*). Data shown in *Panels F and G* are representative of 3 experiments.

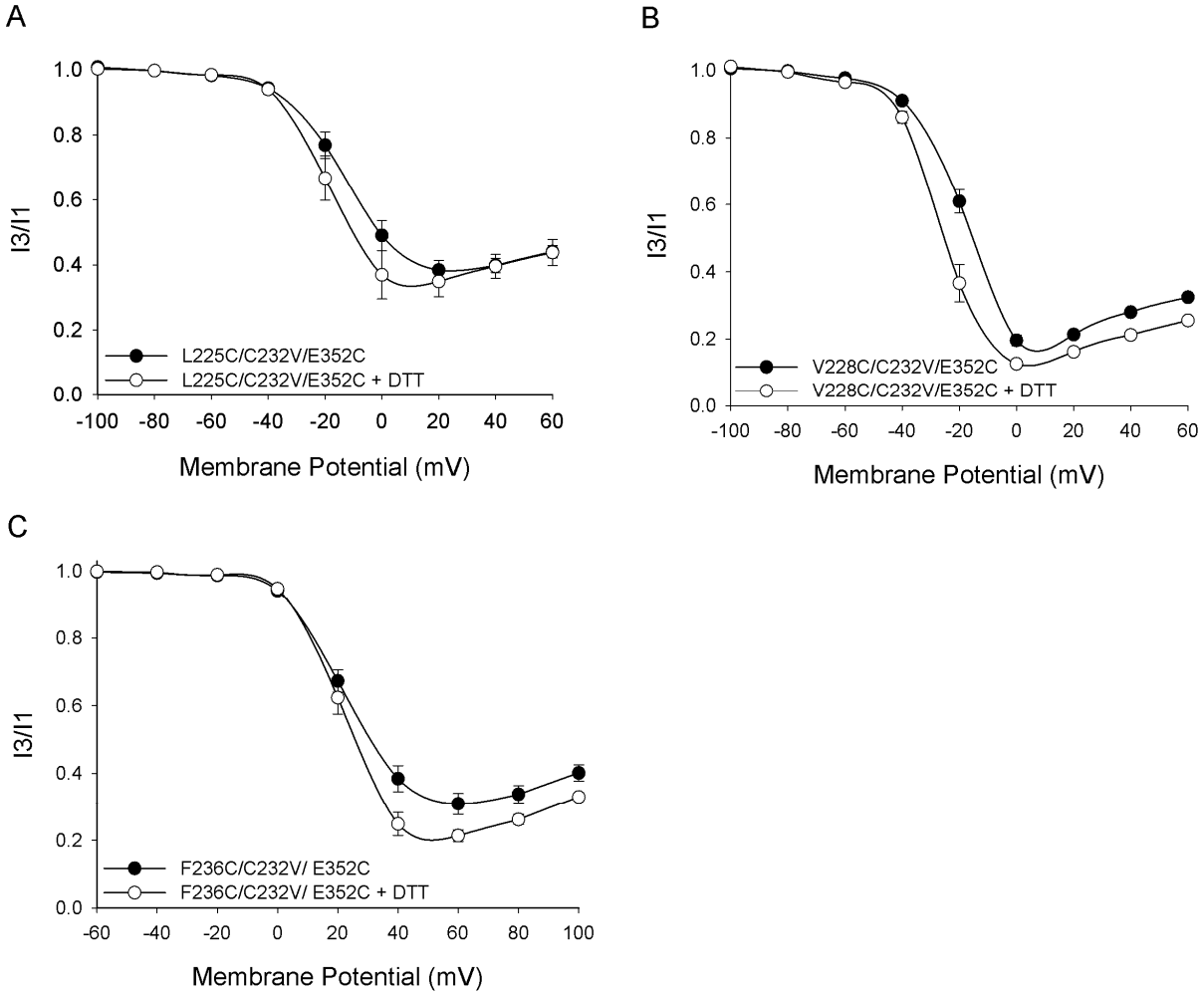

Supplementary Figure S1.

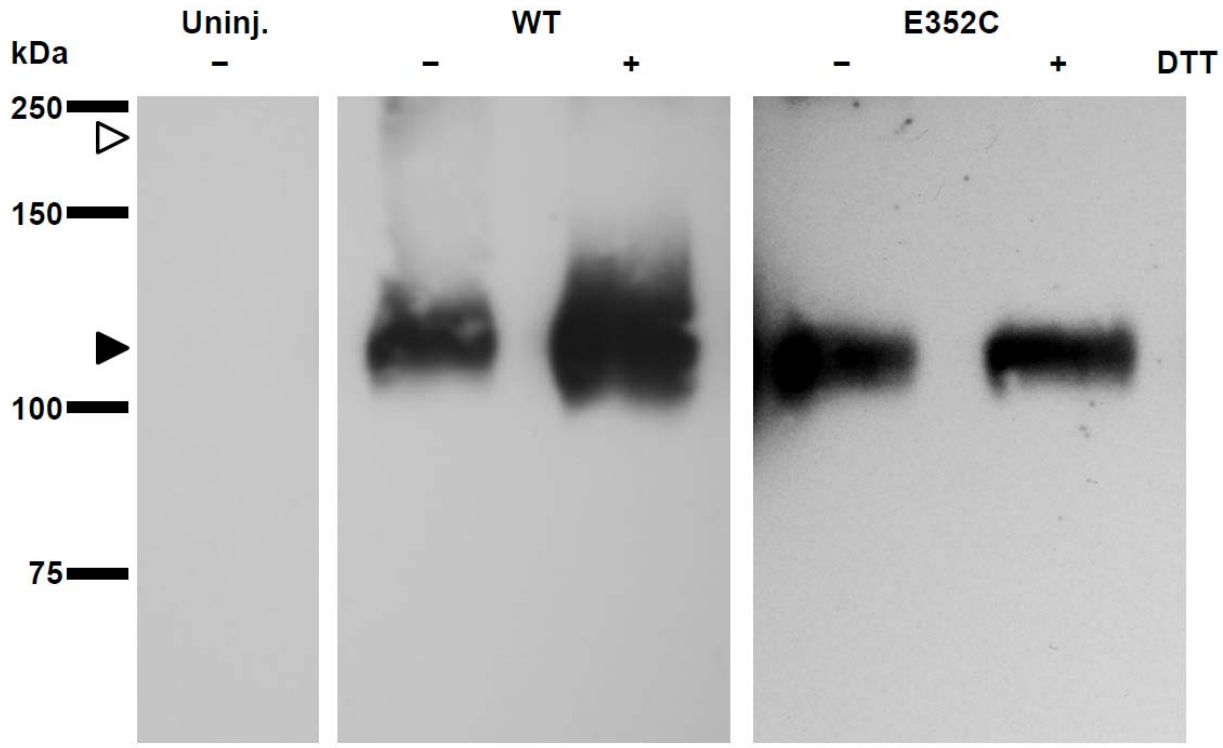

Supplementary Figure S2.

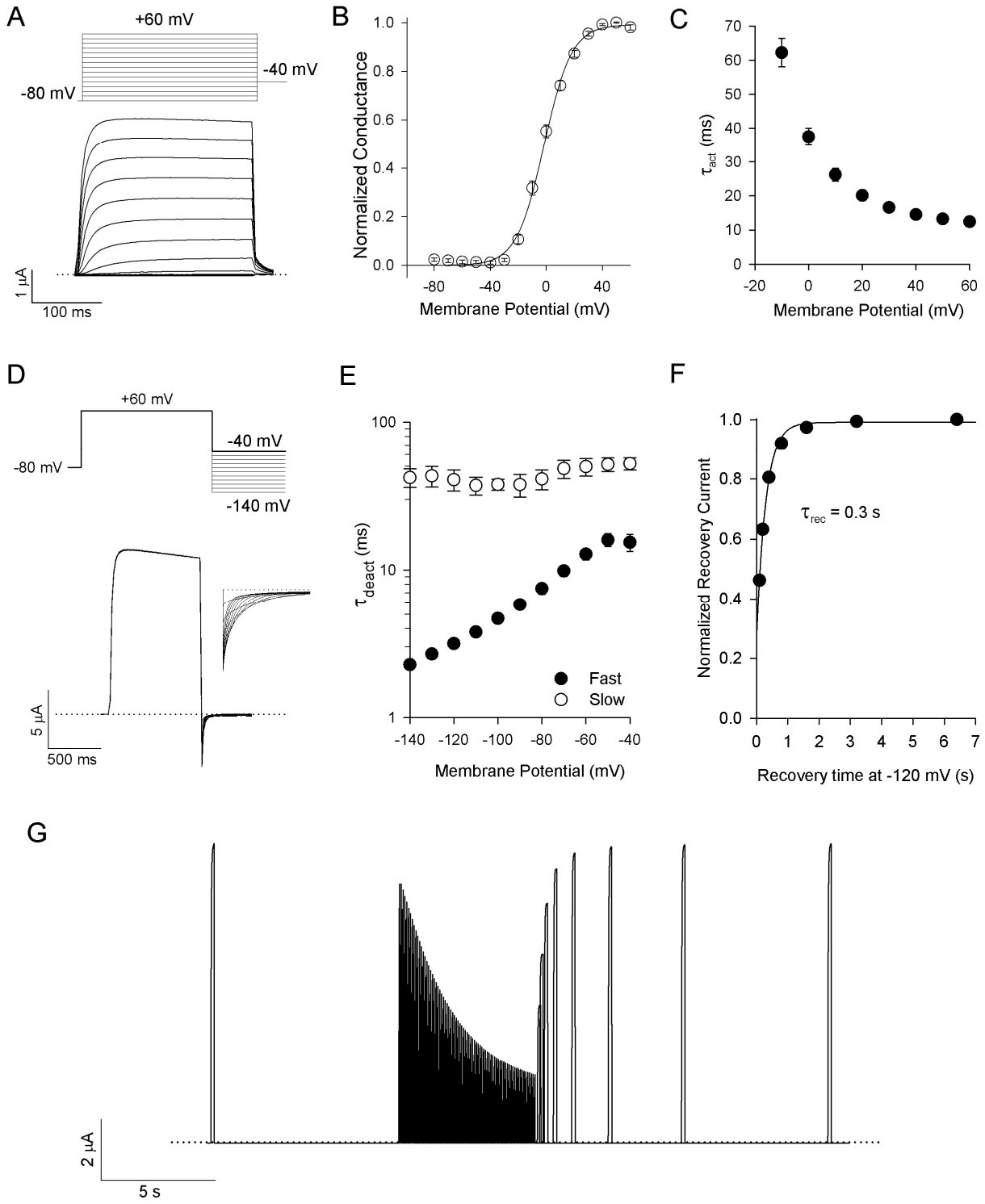

Supplementary Figure S3

Table S1. Summary of gating kinetics used to constrain the gating model for Kv2.1

	wt	E352C	R289C
τ_{act} (ms)*	12.4 ± 1.1 (9)	10.0 ± 1.1 (5)	25.9 ± 2.0 (6)
$\tau_{deact, fast}$ (ms)†	2.8 ± 0.1 (5)	2.8 ± 0.1 (5)	4.6 ± 0.1 (5)
$\tau_{rec, fast}$ (s)‡	0.30 ± 0.01 (3)	0.28 ± 0.01 (5)	6.24 ± 0.47 (5)

* τ_{act} was measured in ND96 during a 300 ms pulse to +60 mV (Fig. S1A, C)

† $\tau_{deact, fast}$ was measured in 30 mM K^+ solution at −140 mV (Fig. S1D, E)

‡$\tau_{rec, fast}$ was measured from a fit of the recovery current following a 5 s pulse train to +60 mV in ND96 (Fig. S1F, G). The interpulse voltage (i.e. between the pulse train and the recovery test pulse) was −120 mV for wt channels and −110 mV for E352C and R289C.

Reference List

1. Juranka, P. F., A. P. Haghighi, T. Gaertner, E. Cooper, and C. E. Morris. 2001. Molecular cloning and functional expression of Xenopus laevis oocyte ATP-activated P2X4 channels. Biochim. Biophys. Acta 1512:111-124.

2. Aziz, Q. H., C. J. Partridge, T. S. Munsey, and A. Sivaprasadarao. 2002. Depolarization induces intersubunit cross-linking in a S4 cysteine mutant of the Shaker potassium channel. J. Biol. Chem. 277:42719-42725.

3. Jiang, M., M. Zhang, I. V. Maslennikov, J. Liu, D. M. Wu, Y. V. Korolkova, A. S. Arseniev, E. V. Grishin, and G. N. Tseng. 2005. Dynamic conformational changes of extracellular S5-P linkers in the hERG channel. J. Physiol 569:75-89.

4. Zhang, H. J., Y. Liu, R. D. Zühlke, and R. H. Joho. 1996. Oxidation of an engineered pore cysteine locks a voltage-gated K^+ channel in a nonconducting state. Biophys. J. 71:3083-3090.